THE TEMPERATURE DRIFT SUPPRESSION OF MODE-LOCALIZED RESONANT SENSORS

*Jiming Zhong, Jing Yang, and Honglong Chang**
MOE Key Laboratory of Micro and Nano Systems for Aerospace,
Northwestern Polytechnical University, Xi'an, China

ABSTRACT

This paper for the first time experimentally demonstrates the temperature drift suppression in the linear measurement range of mode-localized resonant sensors. Based on a mode-localized stiffness sensor, within a temperature range of [290, 350] K with a step of 10 K, the maximum measurement error of the amplitude ratios readout is only 8.9%, while that of frequency shift is 1137%. And the shift of the scale factor of amplitude ratios is only ~11.6% whereas that of the frequency readout is ~61.6%, which verifies that mode-localized sensors own an excellent capability of temperature drift suppression.

INTRODUCTION

Over the past decades, the microelectromechanical systems (MEMS) sensors are widely used in the fields of consumer electronics, automobile safety system, etc. The silicon as one of the most common materials of MEMS sensors, its Young's modulus is highly dependent on temperature, this means any silicon based MEMS sensor is a temperature sensor. Besides, the thermal stress caused by temperature changing will have a great influence on the sensitivity and reliability of sensors, the temperature drift has become one major factor of limiting the measuring precision. In order to reduce the temperature drift, many methods such as temperature control or compensation are proposed to suppress the temperature drift [1], [2]. However, the temperature coefficient of MEMS sensors is not stable and the modeling is difficult, it is hard to eliminate the temperature error by temperature compensation or temperature control.

Recently, the mode localization phenomenon has been used as a novel transduction scheme for enhancing the sensitivity by several orders of magnitude, and varieties of mode-localized sensors with a drastic sensitivity amplification by using the amplitude ratio as the output metric have been presented, such as stiffness sensors [3], electrometers [4], accelerometers [5] and tilt sensors [6]. Especially all of these sensors claim to own good common mode noises (including the temperature and ambient pressure) rejection capability since the temperature variation or the ambient pressure drift affects both numerator and denominator of the amplitude ratio readout theoretically. However, few of them provide enough experimental data to prove it except a preliminary validating in [7] and an experimentally demonstration for the ambient pressure drift rejection capability in [8]. The validations in [7] for the temperature drift suppression are based on the responses of the resonators under only one structure perturbation (0.232N/m). In this work, we for the first time experimentally validate the temperature drift suppression in the linear measurement range of mode-localized sensors. The results show that the temperature drift rejection capability of the amplitude ratio readout is extremely higher than that of the frequency readout.

COMMON MODE NOISES REJECTION THEORY

For the weakly coupled resonators (WCRs) with two degree-of-freedom, the mass-spring-damper model is illustrated in Figure 1. m_1 and m_2 represent the effective mass of two resonators respectively, the effective stiffness of the resonators is k_1 and k_2, x_1 and x_2 represent the displacement of each mass, the damping of each resonator is c_1 and c_2, k_c is the coupling stiffness, F_1 and F_2 represent the driving force.

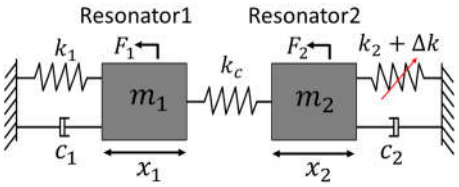

Figure 1: Schematic diagram of the mass-spring-damper model of a 2DoF WCRs.

The dynamic equations of this system can be written as:

$$\begin{aligned} m_1\ddot{x}_1 + c_1\dot{x}_1 + k_1x_1 + k_c(x_1 - x_2) &= F_1 \\ m_2\ddot{x}_2 + c_2\dot{x}_2 + (k_2 + \Delta k)x_2 - k_c(x_1 - x_2) &= F_2 \end{aligned} \quad (1)$$

The mass and stiffness of the two resonators are assumed ideally symmetric, $m_1 = m_1 = m$, $k_1 = k_2 = k = m\omega_0^2$, ω_0 is the eigenfrequency of resonator. Defining the relative stiffness perturbation $\delta = \Delta k/k$, and the coupling factor $\kappa = k_c/k$, thus the equation (1) can be rewritten as:

$$\begin{aligned} \frac{d^2x_1}{dt^2} + \frac{\omega_0}{Q}\frac{dx_1}{dt} + \omega_0^2(1+\kappa)x_1 - \kappa\omega_0^2x_2 &= \frac{F_1}{m_1} \\ \frac{d^2x_2}{dt^2} + \frac{\omega_0}{Q}\frac{dx_2}{dt} + \omega_0^2(1+\kappa+\delta)x_2 - \kappa\omega_0^2x_1 &= \frac{F_2}{m_2} \end{aligned} \quad (2)$$

The transfer functions of the system can be derived as:

$$\begin{aligned} H_1(s) &= s^2 + \frac{\omega_0}{Q}s + \omega_0^2(1+\kappa) \\ H_2(s) &= s^2 + \frac{\omega_0}{Q}s + \omega_0^2(1+\kappa+\delta) \end{aligned} \quad (3)$$

Thus, the equation (2) can be rewritten as:

$$\begin{aligned} H_1(s)X_1(s) - \kappa\omega_0^2x_2 &= \frac{F_1}{m_1} \\ H_2(s)X_2(s) - \kappa\omega_0^2x_1 &= \frac{F_2}{m_2} \end{aligned} \quad (4)$$

Solving (4), the eigenvector (amplitude ratio) of WCRs can be derived as:

$$\frac{X_2}{X_1} = \frac{\kappa\omega_0^2 \cdot F_1 + H_1(s) \cdot F_2}{\kappa\omega_0^2 \cdot F_2 + H_2(s) \cdot F_1} \tag{5}$$

If the damping is ignored, the dynamic equations can be simplified, and the eigenfrequency and amplitude ratio of the WCRs in the ith vibration mode can be written in an even simpler form:

$$\omega_i^2 = (1 + \delta + 2\kappa \mp \sqrt{\delta^2 + 4\kappa^2})\omega_0^2$$
$$AR_i = \frac{X_{2i}}{X_{1i}} = \frac{\delta \pm \sqrt{\delta^2 + 4\kappa^2}}{2\kappa} \qquad i = 1,2 \tag{6}$$

From (6), it can be observed that the amplitude ratio based output metric is a dimensionless parameter, any structural parameters caused by temperature drift will affect both the numerator and denominator, which makes the output of mode-localized sensors virtually immune to temperature variations, whereas the frequency output does not have this common mode rejection capability.

DEVICE FABRACATION

In this paper, a mode-localized stiffness sensor consists of two single-tine resonators which are symmetrically coupled by two mechanical beams is fabricated in a standard SOI technology [9-11] with a structure layer of 30 um thickness. The schematic diagram and SEM picture of the accelerometer is shown in Figure 2.

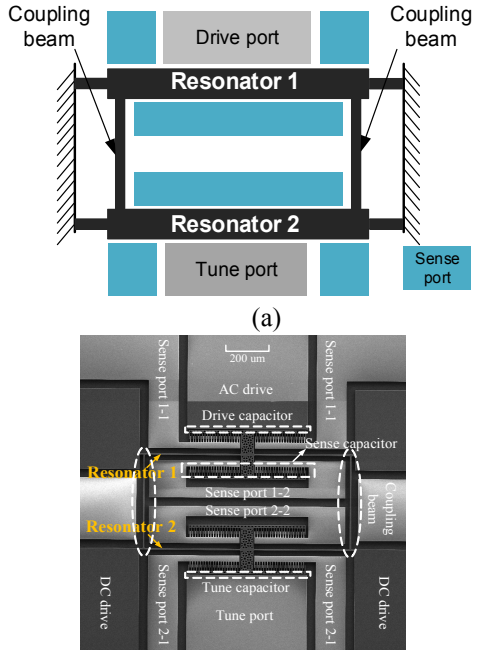

Figure 2: Schematic diagram (a) and SEM image (b) of the mode-localized stiffness sensor

The sense ports are designed at both sides of each tine for differential sensing. The DC bias voltage applied to the tuning port introduces the electrostatic negative stiffness perturbations. The sensing element is packaged in a 20mTorr environment and tested in a drying oven where the temperature can be adjusted.

A similar open loop circuit in [12] is used here, as shown in Figure 3. The signal extraction circuits are placed outside the oven where the ambient temperature is kept at 290K by air-conditioning. In the measurement, a sweep AC signal (100 mVpk) from the dynamic signal analyzer is applied to the drive port when the DC voltage applied to the resonators is 20 V. The amplitude signals are detected by comb capacitors from both sides of each resonator by two charge amplifiers. Instrumentation amplifiers (INAs) are used to realize differential detection and feedthrough elimination. Different stiffness perturbations are added by tuning the DC voltage applied on the tune electrodes, and the stiffness perturbation caused by the potential difference between the tune port and the WCRs can be calculated based on the formula $\Delta k = \varepsilon A V_d^2 / g_0^3$, where $\varepsilon = 8.85 \times 10^{-12}\ F/m$ is the permittivity of vacuum, A is the effective cross-sectional area of the tuning capacitors which is about 16320 μm^2, V_d is the voltage difference between the tuning electrodes and the WCRs, and g_0 is the capacitor gap of 3 μm.

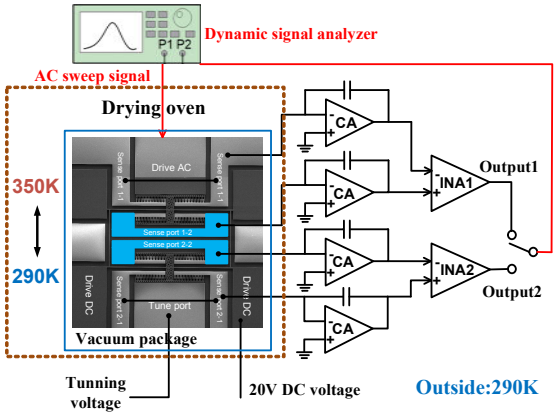

Figure 3: Schematic diagram of the test setup.

TEST RESULTS AND ANALYSIS

In order to verify the temperature drift suppression of the amplitude ratio readout, we recorded the magnitude-frequency responses of Resonator 1 and Resonator 2 with different stiffness perturbations at a temperature of 290K, the results are shown in Figure 4 (a) and (b).

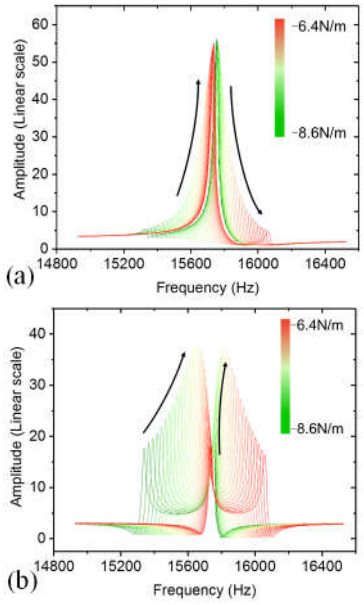

Figure 4. Magnitude-frequency responses of Resonator 1(a) and Resonator 2 (b) versus stiffness perturbation.

The measured veering curves of the amplitude ratios as well as frequency are shown in Figure 5.

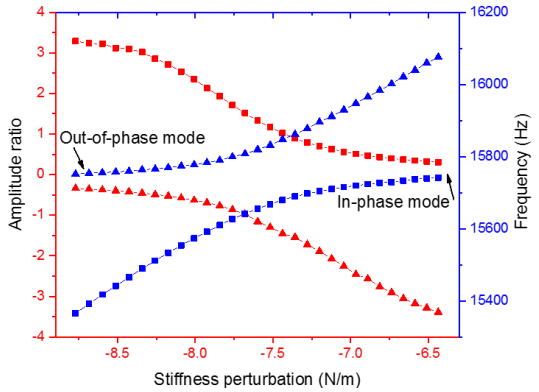

Figure 5. The observed veering curves of the amplitude ratio and frequency at 290(K).

At the veering point, the resonant frequency of the 1st mode (in-phase mode) is about 15665 Hz, and the 2nd mode (out-of-phase mode) is about 15819 Hz. The frequency difference is 154 Hz which means the coupling factor $\kappa = k_c/k = 0.0098$. For the reason of the stiffness disorder of the WCRs caused by the fabrication tolerances, the initial work point of the WCRs is not at veering point. In addition, it can be seen that the better linearity can be obtained from out-of-phase mode, which is chosen as the working mode.

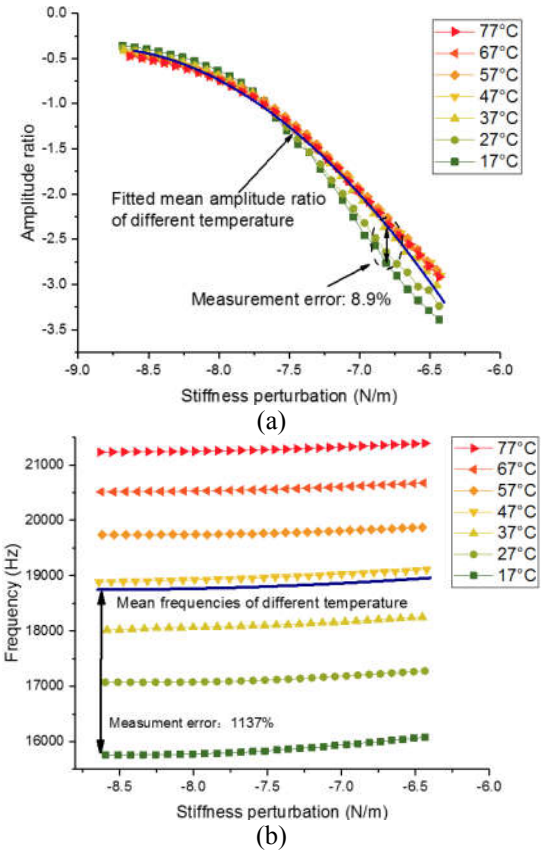

Figure 6. Veering curves of the amplitude ratios (a) and frequency (b) of out-of-phase mode at different temperatures.

As shown in Figure 6, within a temperature range of [290, 350] K with a step of 10 K, the amplitude ratios and frequency of out-of-phase mode with different stiffness perturbations have been tested to compare the influences of the temperature variations to the frequency and amplitude ratio. It can be seen from Figure 6 that the temperature variations can change the frequency dramatically, while that has a negligible effect on the amplitude ratio. Compared to the mean values of different temperature, we respectively calculated measurement error, the maximum measurement error of the frequency (1137% and the simulated value is 986%) is ~127 times higher than that of amplitude ratios (~8.9%) when the simulated measurement error is 7%, which is mainly caused by the asymmetry of the sensor's structure.

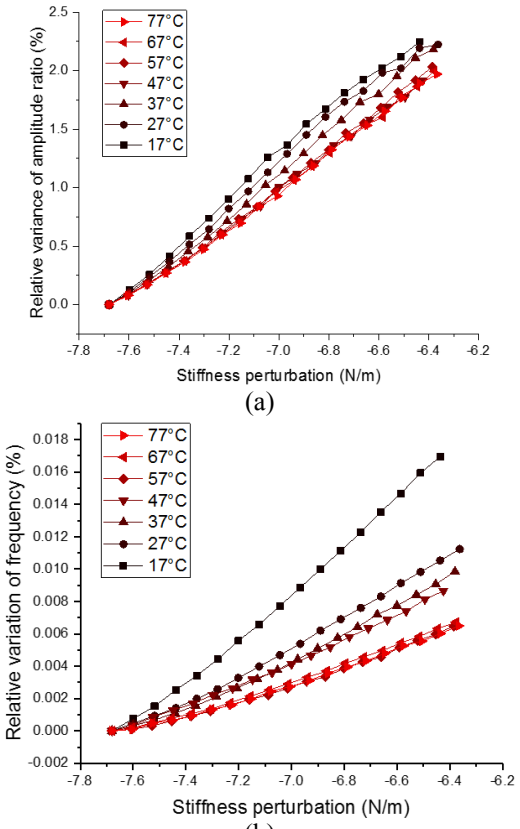

Figure 7. Relative variations of amplitude ratios (a) and frequency (b) at different temperatures.

In order to compare the amplitude and frequency stability, the relative variation of amplitude ratios and resonant frequencies as functions of the stiffness perturbations under operation temperature are tested respectively in the linear measurement range. As the results shown in Figure 7, the scale factor of the frequency readout varies distinctly, while that of amplitude ratios changes slightly. The relative variation of scale factor of amplitude ratios is ~11.6%, while that of the frequency readout is ~61.6% and the amplitude ratio based sensitivity is two orders higher than the frequency based sensitivity for the whole temperature range.

CONCLUSIONS

In this paper, the amazing temperature drift suppression capability in the linear measurement range of

mode-localized resonant sensors is experimentally demonstrated. The experiment results show that the output of frequency is significantly affected by the temperature variations, while that of amplitude ratio is not. The maximum measurement error of the frequency is orders of magnitude higher than that of amplitude ratios, and the relative variation of scale factor of the frequency readout is six times higher than that based on amplitude ratios. They prove that the temperature drift rejection capability of the amplitude ratio readout is extremely higher than that of the frequency readout.

ACKNOWLEDGMENTS

This work was supported by the National Natural Science Foundation of China under Grant 51575454, and the Fundamental Research Funds for the Central Universities 3102017HQZZ009.

REFERENCES

[1] A. Jaakkola, M. Prunnila M, T. Pensala, J. Dekker and P. Pekko, "Determination of doping and temperature-dependent elastic constants of degenerately doped silicon from MEMS resonators". *IEEE transactions on ultrasonics, ferroelectrics, and frequency control 61(7)*, pp. 1063-1074, 2014.

[2] J. Zhang, A. Qiu, Q. Shi, Y. Bian and G. Xia, "Research on temperature compensation method of silicon resonant accelerometer based on integrated temperature measurement resonator". *In Electronic Measurement & Instruments (ICEMI),* Vol. 3, pp. 1577-1581, 2015.

[3] C. Zhao, G.S. Wood, J. Xie, H. Chang, S. H. Pu, M. Harold, H. Chong, and M. Kraft, "A sensor for stiffness change sensing based on three weakly coupled resonators with enhanced sensitivity". *In IEEE 28th International Conference on Micro Electro Mechanical Systems,* Jan 18-22, 2015, pp. 18-22.

[4] H. Zhang, W. Yuan, J. Huang, B. Li, and H. Chang. "A high-sensitive resonant electrometer based on mode localization of the weakly coupled resonators". *In IEEE 29th International Conference on Micro Electro Mechanical Systems*, Jan 22-26, 2016, pp. 938-941.

[5] H. Zhang, J. Huang, W. Yuan, and H. Chang. "An Acceleration Sensing Method Based on the Mode Localization of Weakly Coupled Resonators". *Journal of Microelectromechanical Systems.* vol. 25, no. 5, pp. 937-946, 2016

[6] B. Li, H. Zhang, J. Zhong, and H. Chang, "A mode localization based resonant MEMS tilt sensor with a linear measurement range of 360°". *in Proc. 29th IEEE Int. Conf. Micro Electro Mech. Syst.*, Shanghai, China, Jan. 2016, pp. 938–941.

[7] P. Thiruvenkatanathan, J. Yan, A. A. Seshia, "Differential amplification of structural perturbations in weakly coupled MEMS resonators". *IEEE Transactions on Ultrasonics, Ferroelectrics, and Frequency Control.* vol.57, no.3, pp: 690-7. Mar. 2010.

[8] H. Zhang, J. Zhong, W. Yuan, J. Yang, and H. Chang. "Ambient pressure drift rejection of mode-localized resonant sensors". In IEEE 30th International Conference on Micro Electro Mechanical Systems, Jan 22-26, 2017, pp. 1095-1098.

[9] H. Chang, J. Xie, Q. Fu, Q. Shen, and W. Yuan, "Micromachined inertial measurement unit fabricated by a SOI process with selective roughening under structures". *IET Micro & Nano Letters*, vol. 6, no. 7, pp. 486–489, Jul. 2011.

[10] Y. Hao, J. Xie, W. Yuan, H. Chang. "Dicing-free soi process based on wet release technology". *Micro & Nano Letters*, vol. 11, no. 11, pp. 775-778, Nov. 2016

[11] Y. Hao, W. Yuan, J. Xie, Q. Shen, H. Chang, "Design and verification of a structure for isolating packaging stress in SOI MEMS devices". *IEEE SENSORS JOURNAL*, vol. 17, no. 5, March 1, 2017

[12] H. Zhang, W. Yuan and H. Chang, "Characterization of forced localization of disordered weakly coupled micromechanical resonators" *Microsystems & Nanoengineering* (2017) 3, 17023

CONTACT

*Honglong Chang, changhl@nwpu.edu.cn